

Multi-spacecraft Investigation of ICME-driven Interplanetary Shock Interaction on the Solar Wind Turbulence in the Inner Heliosphere

B. Park, A. Pitňa, J. Šafránková, Z. Němeček, and P. Basuvaraj

Charles University, Faculty of Mathematics and Physics, Prague, Czech Republic.

Abstract. Recent space missions enable multi-point analysis of solar wind turbulence in the inner heliosphere. We identify an ICME event in March 2022, and estimate changes of spectral properties such as spectral index, magnetic helicity, and magnetic compressibility across an ICME-driven shock using the spacecraft of Solar Orbiter, ACE, DSCOVR, and Wind. Another ICME event identified by *Trotta et al.* [2023] is adopted for the comparison of these properties. Despite a small number of events leading to inconclusive results of evolution with the heliocentric distance, several common trends are observed in both cases: little change of spectral steepness, decreasing jump of magnetic helicity and compressibility, and increasing power enhancement of fluctuations from up- to downstream with the heliocentric distance. However, for a deeper insight on the nature of the radial propagation of these parameters, statistical analyses with a larger number of events are essential.

Introduction

Interplanetary coronal mass ejections (ICMEs), the large-scale structures of dynamically evolving plasma and magnetic field from the Sun and extending into interplanetary space, have been of a significant scientific interest due to their influence on space weather [e.g., von Steiger and Richardson, 2006]. ICMEs have been observed with a set of coronagraph images from the Large Angle Spectroscopic Coronagraph (LASCO) [Brueckner et al., 1995] at the Solar and Heliospheric Observatory (SOHO) spacecraft allowing the estimation of ICME expansion speed and acceleration [Maunder et al., 2022]. Observed CME events are listed in SOHO LASCO CME catalog. However, not all ICMEs are observed by this coronagraph due to the projection effect [Howard and Tappin, 2009]. By analyzing the *in-situ* measurements of plasma parameters (i.e., magnetic field, proton velocity, and proton density profiles), the ICME observations can be supplemented. The observations of ICME events usually exhibit several distinctive structures; shock, sheath, and magnetic flux rope [Kilpua et al., 2017]. The magnetic flux rope contains a smooth rotation of the magnetic field and a relatively low proton density, and the ICME-driven shocks are identified with a sudden jump in the magnetic field, velocity, and density. The sheath region is between these two structures.

Interplanetary (IP) shocks propagating through the heliosphere lead to plasma heating and compression, and their complex properties often vary with distance [Pérez-Alanis et al., 2023]. Recent space missions such as Solar Orbiter, Parker Solar Probe, Juno and Wind facilitate multi-point *in-situ* measurements of solar wind turbulence at different locations of the heliosphere. In order to investigate the evolution of the shock properties, tracking an individual IP shock is required using these spacecraft. As presented in *Lugaz et al.* [2018] and references therein, many multi-spacecraft analyses have been conducted with diverse angular separations and at different heliocentric distances. The recent study by *Möstl et al.* [2022] identifies a large number of ICMEs, and the events are listed in the HELIO4CAST ICME catalog.

Despite the wealth of knowledge on this topic, understanding the nature of ICME-driven shocks, such as the evolution of the magnetic field fluctuations, helicity, and compressibility altering with heliodistance still holds a gap. Our study aims further investigation of the complexities of the interactions between IP shocks and turbulence varying with distance from the Sun. We analyze an ICME event observed from Mar-11 to Mar-13, 2022 (2022-Mar, hereinafter) by Solar Orbiter, Advanced Composition Explorer (ACE), Deep Space Climate Observatory (DSCOVR), and Wind. We compare this ICME event with another event, Nov-03, 2021 identified by *Trotta et al.* [2023] (2021-Nov, hereinafter). In the section of Methods, we outline the data sources and methodology employed in our investigation. Next, a detailed analysis of the spectral properties of the magnetic field fluctuations, magnetic helicity, magnetic compressibility, and their dependencies on heliodistance are presented. A deeper discussion of the results and the conclusion of this study follow in the last section.

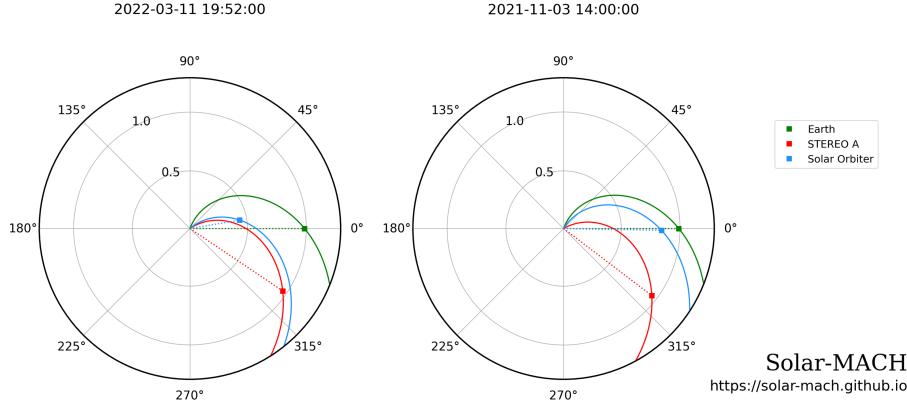


Figure 1. Positions of the Earth (green square), STEREO-A (red square), and Solar Orbiter (blue square) at 19:52:00 on March 11, 2022 (left panel), and at 14:00:00 on November 03, 2021 (right panel) in the Stonyhurst heliographic coordinate system. Solid and dotted lines connected from the Sun represent spiral magnetic fields and radial propagation, respectively. ACE, DSCOVR, and Wind are assumed to be near the Earth (at L1).

Methods

Estimation of the evolution of ICME-driven IP shocks needs the spacecraft located at different distances in the heliosphere. The timing of radial alignments for various spacecraft are calculated by *Telloni* [2023], and the detailed positions of the spacecraft can be checked with the open-source Solar MAGnetic Connection Haus tool (Solar-Mach) [*Gieseler et al.*, 2023]. Figure 1 (left) presents the positions of the near-Earth spacecraft (green square), STEREO-A (red square) and Solar Orbiter (blue square) in the Stonyhurst heliographic coordinate system at 19:52 on 2022-03-11 (2022-Mar) and at 14:00 on 2021-11-03 (2021-Nov, right panel). In the event of 2022-Mar, Solar Orbiter is located at approximately 0.44 au and the spacecraft relatively fixed at the first Lagrangian point (L1) near the Earth at 1 au (ACE, DSCOVR, and Wind) are expected to measure the same radially expanding plasma, while Solar Orbiter is radially aligned with L1 at 0.84 au in 2021-Nov. The longitudinal separation of STEREO-A is 34° and 37° for 2022-Mar (left) and 2021-Nov (right), respectively. Based on a qualitative comparison of plasma parameters with those from the other spacecraft shown in Figure 2, STEREO-A seems encountering the same ICME event due to its expansion with distance. However, the properties of shocks driven by the ICME could deviate at such a large longitudinal separation. Thus, a shock detected by STEREO-A is not included in this study, anyway its magnetic field components, proton velocity, and number density are shown in Figure 2 for comparison.

Profiles of the magnetic field, velocity, and density which include ICME structures such as shock, sheath, and magnetic flux rope from the noon of March-10 to the noon of March-15 in 2022 (2022-Mar) are presented in Figure 2. The identification of the shocks represented as cyan dotted lines are based on a methodology from *Krupařová et al.* [2013]. The velocity and density from ACE and DSCOVR are not shown due to unavailability of the data in the given time interval. Magnetic field data are measured by the fluxgate vector magnetometer (MAG) instrument at Solar Orbiter [*Horbury et al.*, 2020], the Magnetic Field Instrument (MFI) of 1-s resolution at ACE [*Smith et al.*, 1998], the magnetometer instrument with 1-s resolution at DSCOVR [*Szabo et al.*, 2016], the In situ Measurements of Particles and CME Transients (IMPACT) suite at STEREO-A [*Luhmann et al.*, 2008], and the Magnetic Field Instrument (MFI) with 92-ms resolution at WIND [*Lepping et al.*, 1995]. The velocity, density, and temperature are measured by the Solar Wind Analyser (SWA) at Solar Orbiter [*Owen et al.*, 2020], the Plasma and Suprathermal Ion Composition (PLASTIC) instrument at STEREO-A [*Galvin et al.*, 2008], and the Solar Wind Experiment (SWE) instrument at Wind [*Ogilvie et al.*, 1995].

In order to analyze the shock parameters, we adopt 15-minute intervals prior to and after the shock crossing as upstream and downstream, respectively, skipping 5 minutes in the shock vicinity to avoid near-shock wave activities and instabilities driven by reflected particles [*Lalti et al.*, 2022]. The shock normal is estimated by the magnetic coplanarity theorem [*Paschmann and Daly*, 1998], and the angle between the normal and average upstream magnetic field is indicated as θ_{Bn} . The power spectral densities (PSDs) of the magnetic field fluctuation components are analyzed by the continuous wavelet transform (CWT) with a Morlet wavelet ($\omega_0 = 6$) [*Torrence and Compo*, 1998] in 3-hour intervals for up- and downstream omitting 5 minutes from the shock vicinity. The spectral index α in the inertial range is determined by a linear fit of the PSD with the minimization of χ squared in the frequency range of [0.003, 0.03 Hz], and the change of the spectral index across the shock (marked with the superscript as “up” and “down”, respectively) is labeled as a ratio, $R_\alpha = \alpha^{\text{down}}/\alpha^{\text{up}}$. The normalized magnetic helicity, $\sigma_M = 2\text{Im}(\tilde{B}_T^* \tilde{B}_N)/(\tilde{B}_R^2 + \tilde{B}_T^2 + \tilde{B}_N^2)$ is the measure of handedness of the magnetic field

fluctuations where the direction of the average magnetic field is “rectified” by multiplying a negative sign when it points outward the Sun, so that a positive value corresponds to right-handedness and a negative value for left-handedness. $\tilde{B}_{R,T,N}$ are the elements of the wavelet transformed energy spectral tensor in the RTN-coordinate system. Magnetic compressibility, C_B which is the amount of compressible fluctuations in the total fluctuations is computed as the ratio between the PSD of the magnetic field magnitude and total magnetic field fluctuations, $C_B = \text{PSD}_{|B|}/\text{PSD}_B$. The changes of σ_M and C_B from up- to downstream are determined as ratios between their up- and downstream median values $|R_{MH}|$ and R_{C_B} , respectively, within the inertial range of 0.003–0.03 Hz. The median value of the power enhancement of magnetic field fluctuations in the inertial range is marked as R_{PSD} .

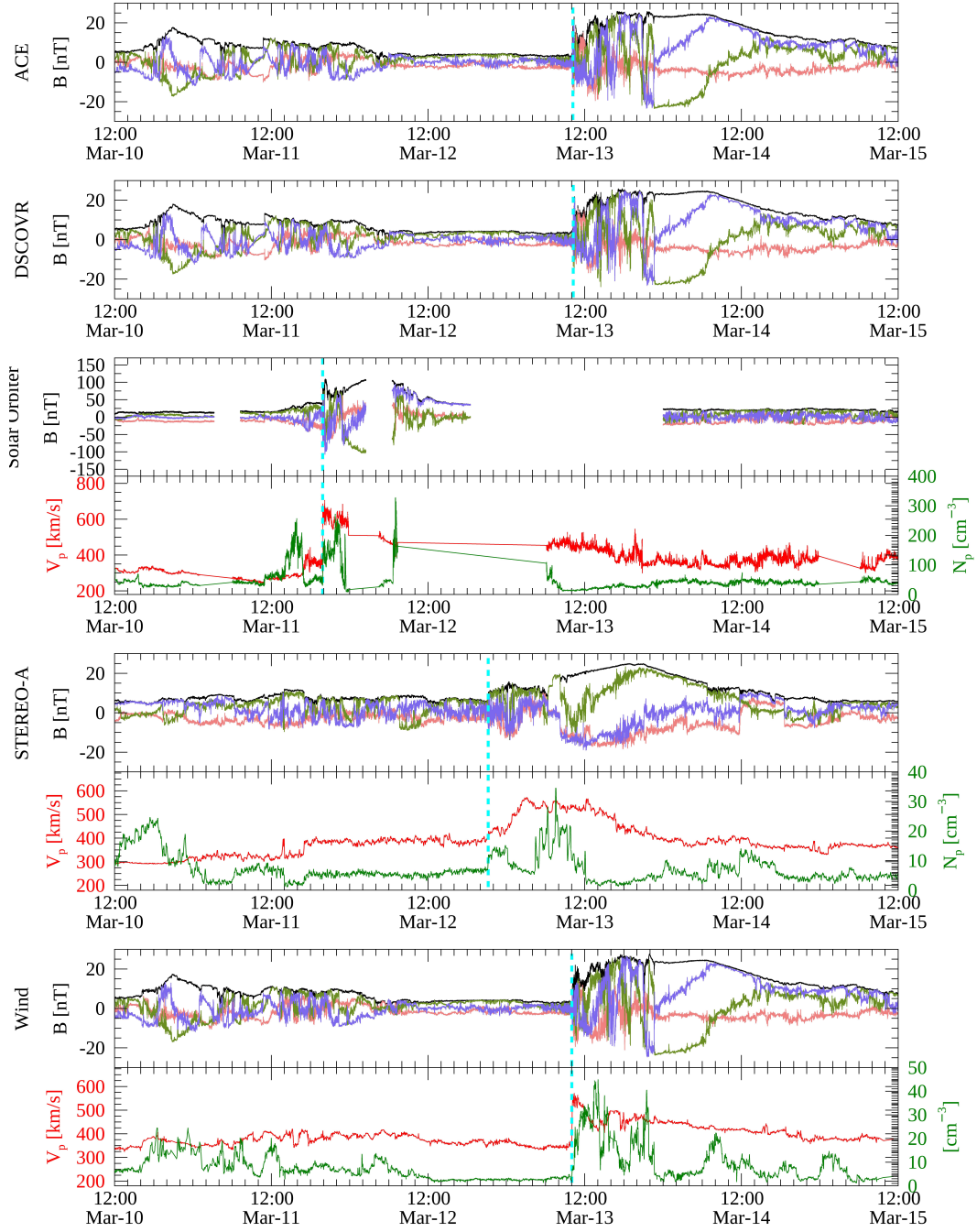


Figure 2. Profiles of solar wind parameters (B , V_p , and N_p) from the noon of March 10 to the noon of March 15 in the year of 2022. Magnetic fields are measured in the RTN coordinate system (pink for radial, light green for tangential, and light blue for normal components). V_p and N_p are represented by red and green solid lines, respectively. Identified shocks are represented by cyan dotted lines. Even though plasma data from ACE and DSCOVR are not available in this time interval, the shocks are identified based on the Wind observation.

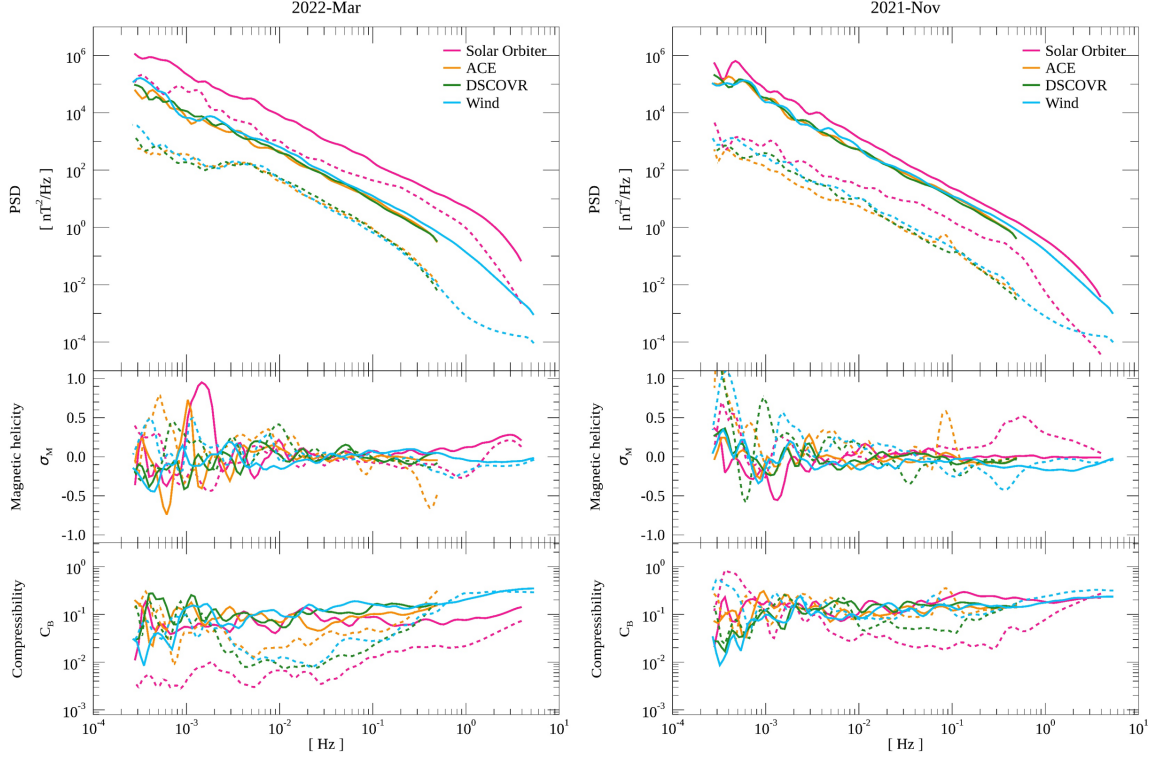


Figure 3. PSD (top panels), magnetic helicity σ_M (middle panels), and magnetic field compressibility C_B (bottom panels) observed by Solar Orbiter, ACE, DSCOVR, and Wind in 2022-Mar (left panels) and 2021-Nov (right panels). Up- and downstream spectra are presented as dotted and solid lines, respectively.

Estimation of shock properties at different heliodistances

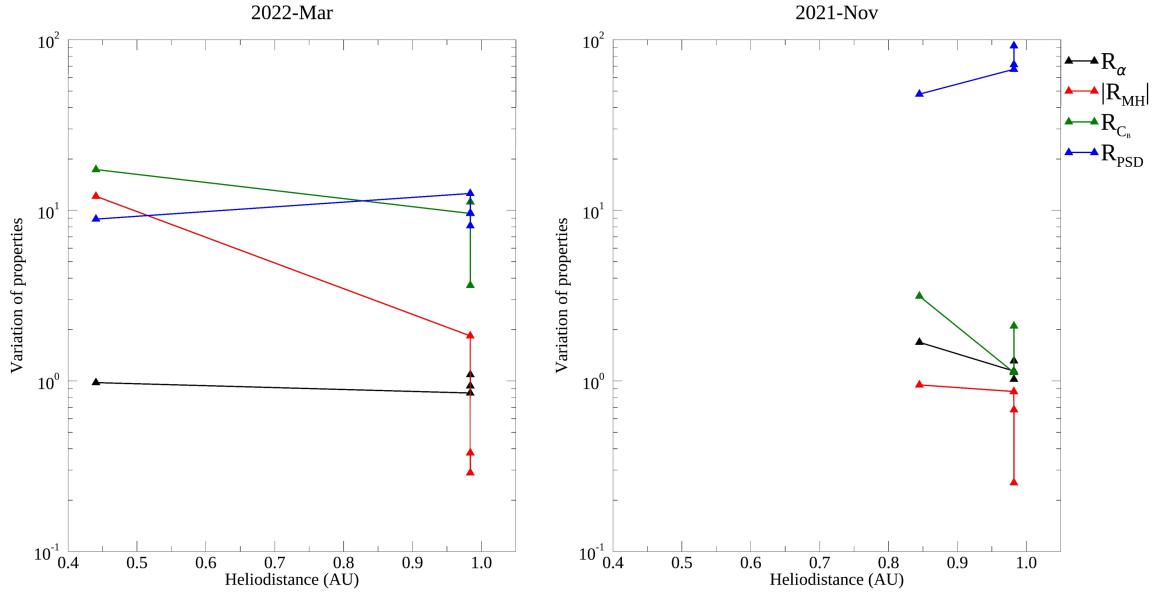
Spectra of the magnetic field fluctuations, magnetic helicity, and magnetic compressibility across ICME shocks derived from Solar Orbiter, ACE, DSCOVR, and Wind observations on 2022-Mar are shown in the left panels and the event of 2021-Nov in the right panels of Figure 3. The up- and downstream PSDs are presented with the dotted and solid lines. Solar Orbiter was closer to the Sun in both cases (0.44 and 0.84 au, respectively) and observes a higher power of the magnetic field fluctuations with a less steep inertial range spectral slope in the up- and downstream than the spacecraft near 1 au (Figure 3 top panels). This result is in agreement with Šafránková *et al.* [2023] presenting a larger power and a smaller inertial range spectral index at closer distances to the Sun. The magnitude of σ_M in the 2022-Mar event (Figure 3 left middle panel) exhibits increase in the 0.2–2 Hz range, while they present a flatter spectra within the inertial range. Additionally, the σ_M spectra in this frequency range (0.2–2 Hz) measured by ACE and Solar Orbiter show a clear change across the shock, suggesting a small structure or wave activity in turbulence decay by shock. On the other hand, in the case of 2021-Nov (Figure 3 right middle panel), significant variations of σ_M across the shock are observed in a similar frequency range (0.07–1 Hz) by ACE, Wind, and Solar Orbiter. As the dependence of C_B on distance is reported by Chen *et al.* [2020], the lowest level of the C_B spectrum in the upstream is observed by Solar Orbiter, the nearest spacecraft to the Sun, in both 2022-Mar (Figure 3 left bottom panel) and 2021-Nov events (Figure 3 right bottom panel) within the inertial range, and upstream C_B from the other spacecraft are similar. The C_B spectra transmitted to the downstream of shock show a different tendency which might be associated with other shock properties rather than with distance. Further analysis of this point will be treated in the discussion section.

The variations of the shock properties, *i.e.*, the change of the inertial spectral index R_α , magnetic helicity $|R_{MH}|$, magnetic compressibility R_{C_B} , and fluctuation power R_{PSD} with distance from the Sun, are presented in Figure 4. Comparing average values measured at L1 by Solar Orbiter observations, a few common trends with distance between 2022-Mar and 2021-Nov can be seen. R_α remains approximately unity in 2022-Mar with distance, which implies that the modification of energy dissipating mechanism for the magnetic field fluctuation by the IP shock is not observed up to 1 au. In 2021-Nov, R_α measured by Solar Orbiter is markedly larger (1.68) than that from the other spacecraft. The upstream spectrum for this event presented in Figure 3 shows a small bump, which can cause a shallower upstream spectral index. It is reasonable to state that IP shocks do not modify the turbulence dissipation with distance if spectral bumps are not considered. $|R_{MH}|$, and R_{C_B}

Table 1. Ratios of the average upstream and downstream turbulent parameters.

Spacecraft	Heliodistance (au) (1)	Shock arrival (UT) (2)			
Solar Orbiter	0.44 [0.84]	19:52:23 2022-Mar-11 [14:04:26 2021-Nov-03]			
Wind	0.98 [0.98]	10:01:26 2022-Mar-13 [19:35:01 2021-Nov-03]			
ACE	0.98 [0.98]	10:11:14 2022-Mar-13 [19:24:05 2021-Nov-03]			
DSCOVR	0.98 [0.98]	10:14:29 2022-Mar-13 [19:24:50 2021-Nov-03]			
	$\theta_{Bn}(\circ)$ (3)	R_α (4)	$ R_{MH} $ (5)	R_{CB} (6)	R_{PSD} (7)
Solar Orbiter	30.2 [45.3]	0.98 [1.68]	12.09 [0.95]	17.34 [3.14]	8.88 [47.98]
Wind	19.8 [33.1]	0.85 [1.14]	1.84 [0.87]	9.59 [1.12]	12.56 [67.13]
ACE	6.9 [9.6]	0.94 [1.31]	0.29 [0.25]	3.63 [1.13]	9.65 [92.19]
DSCOVR	5.7 [13.3]	1.09 [1.02]	0.38 [0.68]	11.21 [2.10]	8.12 [71.52]
L1 average	10.8 [18.7]	0.96 [1.16]	0.84 [0.60]	8.14 [1.45]	10.11 [76.95]

Note. The values outside brackets are computed for the event of 2022-Mar, while the 2021-Nov values are inside the brackets. From column (4)–(7), the change of parameters are represented as ratios between up- to downstream values. The row of “L1 average” indicates the average values measured by ACE, DSCOVR, and Wind.


Figure 4. Variations of the ratios R_α , $|R_{MH}|$, R_{CB} , and R_{PSD} for the events of 2022-Mar (left panels) and 2021-Nov (right panels).

show a common decreasing trend with distance in both 2022-Mar and 2021-Nov. The $|R_{MH}|$ trend suggests that magnetic field fluctuations in the downstream compared to upstream becomes less helical with distance. The compressive component of magnetic field fluctuations in the solar wind increases with distance, whereas R_{CB} shows the opposite tendency. On the other hand, R_{PSD} , the power enhancement of fluctuations, is positively correlated with the distance from the Sun. This implies that the greater dissipation of turbulent magnetic energy by shock is observed in a larger distance. *Smith et al.* [2001] study the heating of solar wind by the dissipation of magnetic fluctuations, suggesting a potential relation between the power enhancement and plasma heating by shock. However, the demonstration of this relation is not simple. The entropy increase is observed across shock [*Borovsky, 2020*], and a greater increase with a farther heliospheric location is found [*Adhikari et al., 2020*]. Even though the entropy increases monotonously with distance, proton temperature in the solar wind does not. Thus, the association of the evolution of R_{PSD} with the plasma heating by shock as a function of the heliocentric distance remains unsolved. All mentioned values are summarized in Table 1.

Discussion and Conclusion

We focus on the evolution of the interaction of ICME-driven shocks with solar wind turbulence at different distances. We estimate various quantities such as spectral properties of the magnetic field fluctuations and plasma parameters in the up- and downstream of two ICME-driven shocks, 2022-Mar and 2021-Nov. This study intrinsically has a limitation connected with a small number of cases to derive conclusive results. Nevertheless, common trends of variations of parameters with distance are observed: 1) little change in the spectral index, 2) the decreasing magnetic compressibility and helicity change, and 3) increasing power enhancement across shock with the heliocentric distance. As previously stated, these trends are obtained by averaging values at 1 au (measured from ACE, DSCOVR, and Wind), containing a further question; which one is a true value representing properties at a certain distance. Due to lack of *in-situ* observations, the decision of such values inevitably faces difficulty. In this context, we use their averages as a reasonable number for 1 au in our estimation.

The change of C_B in the heliosphere studied in *Shi et al.* [2021] suggests that solar wind turbulence is more Alfvénic closer to the Sun. Furthermore, the decay of compressible fluctuations of the magnetic energy with heliodistance follows a lower rate than that of total fluctuations, which results in the increase of the magnetic compressibility in farther distances from the Sun [*Šafránková et al.*, 2023]. This is indicated in the C_B spectra in Figure 3. The shocks compress plasma turbulence and their strength enlarges with the heliocentric distance [*Pérez-Alanis et al.*, 2023]. Decreasing R_{C_B} with the heliodistance indicates that the effect of the shock strength on C_B is not directly associated with the increase of compressible fluctuations in the downstream, or the amount of these fluctuations in plasma is governed by another condition which compensates the shock intensity such as the upstream Alfvénicity. A statistical study with a larger number of cases is required for more precise estimation of the compressibility transmission through shocks at different heliodistances.

It is important to check whether all spacecraft observe the same IP shocks driven by the ICME. The angles between the mean magnetic field and shock normal θ_{Bn} are presented in column (3) in Table 1. As reported in *Zhao et al.* [2021] analyzing an ICME-driven shock with Solar Orbiter and Wind, θ_{Bn} is expected to increase with distance as the ICME propagates. However, θ_{Bn} becomes lower at 1 au in our cases. *Trotta et al.* [2023] using five L1 spacecraft show the θ_{Bn} decrease. Although statistically significant trends cannot be exhibited as only two cases are considered, the variation of θ_{Bn} could result from the locally rippled shock surface as *Zank et al.* [2021] suggest. As presented in Figure 1, Solar Orbiter and L1 fleet spacecraft are well aligned, suggesting they are expected to observe the same radially propagating shock. The investigation of the θ_{Bn} evolution with distance requires more events observed at different locations.

We adopt 3-hour up- and downstream intervals from the shock crossing for all spacecraft. The downstream plasma measured at Solar Orbiter is far away from the shock crossing at L1 which could be already transmitted to the magnetic cloud of ICME. Even though estimating the parameters of the same propagating plasma is recommended, plasma within the magnetic cloud cannot be used for our analysis considering its distinctive properties such as low beta. Thus, as a caveat, we may compare slightly different up and downstream plasmas observed by multiple spacecraft.

Our study provides further insights into the evolution of spectral properties of magnetic field fluctuations, magnetic helicity, magnetic compressibility, and power spectral density across ICME-driven shocks. We quantify their changes in the inertial range as a ratio of the downstream average quantities to those of upstream. Additionally, in order to estimate the evolution of the changes across shocks with heliodistance, we employ data from the multiple spacecraft, *i.e.*, Solar Orbiter, ACE, DSCOVR, and Wind at different locations in the inner heliosphere. Due to a small number of events (2022-Mar and 2021-Nov), we do not observe a significant relation of the shock property with the heliocentric distance. However, the insignificant change of spectral index, decreasing magnetic helicity and compressibility changes, and increasing power enhancement across the ICME-driven shock with distance are commonly found in both 2022-Mar and 2021-Nov events. The present study should be considered as a preparatory phase for more complex study that will be based on much larger number of shocks observed in a broader range of heliospheric distances, and its main aim is to identify caveats that such study can encounter.

Acknowledgments. The authors thank all Solar Orbiter, STEREO, Wind, ACE, and DSCOVR spacecraft research teams for the magnetic field and plasma data. All data adopted in this study is available at the Coordinated Data Analysis Web (CDAWeb) (<http://cdaweb.gsfc.nasa.gov/cdaweb/>). The authors acknowledge the use of the SOHO LASCO CME catalog (https://cdaw.gsfc.nasa.gov/CME_list/), and HELIO4CAST interplanetary coronal mass ejection (ICME) catalog (<https://heliopforecast.space/icmecat>). The authors also acknowledge the use of the Solar MAgnetic Connection Haus (Solar-MACH) tool (<https://solar-mach.github.io/>). The present work is supported by the Czech Science Foundation under contract 23-06401S and the Charles University Grant Agency under contract 280423 and 256323.

References

- Adhikari, L., Zank, G. P., Zhao, L.-L., and Webb, G. M., Evolution of entropy in the outer heliosphere, *Journal of Physics: Conference Series*, 1620, 012 001, 2020.
- Borovsky, J. E., A statistical analysis of the fluctuations in the upstream and downstream plasmas of 109 strong-compression interplanetary shocks at 1 au, *Journal of Geophysical Research: Space Physics*, 125, e2019JA027 518, e2019JA027518 2019JA027518, 2020.
- Brueckner, G., Howard, R., Koomen, M., Korendyke, C., Michels, D., et al., The large angle spectroscopic coronagraph (LASCO), *Solar Physics*, 162, 357–402, 1995.
- Chen, C. H. K., Bale, S. D., Bonnell, J. W., Borovikov, D., Bowen, T. A., et al., The evolution and role of solar wind turbulence in the inner heliosphere, *The Astrophysical Journal Supplement Series*, 246, 53, 2020.
- Galvin, A., Kistler, L., Popecki, M., Farrugia, C., Simunac, K., et al., The plasma and suprathermal ion composition (PLAS-TIC) investigation on the stereo observatories, *Space Science Reviews*, 136, 437–486, 2008.
- Gieseler, J., Dresing, N., Palmroos, C., Freiherr von Forstner, J. L., et al., Solar-mach: An open-source tool to analyze solar magnetic connection configurations, *Frontiers in Astronomy and Space Sciences*, 9, 2023.
- Horbury, T. S., O'Brien, H., Carrasco Blazquez, I., Bendyk, M., Brown, P., et al., The Solar Orbiter magnetometer, *Astronomy and Astrophysics*, 642, A9, 2020.
- Howard, T. A. and Tappin, S. J., Interplanetary Coronal Mass Ejections Observed in the Heliosphere: 1. Review of Theory, *Space Science Reviews*, 147, 31–54, 2009.
- Kilpua, E., Koskinen, H. E. J., and Pulkkinen, T. I., Coronal mass ejections and their sheath regions in interplanetary space, *Living Reviews in Solar Physics*, 14, 5, 2017.
- Krupařová, O., Maksimovic, M., Šafránková, J., Němeček, Z., Santolík, O., and Krupař, V., Automated interplanetary shock detection and its application to Wind observations, *Journal of Geophysical Research Space Physics*, 118, 4793–4803, 2013.
- Lalti, A., Khotyaintsev, Y. V., Graham, D. B., Vaivads, A., Steinvall, K., et al., Whistler waves in the foot of quasi-perpendicular supercritical shocks, *Journal of Geophysical Research: Space Physics*, 127, e2021JA029 969, 2022.
- Lepping, R. P., Acuña, M. H., Burlaga, L. F., Farrell, W. M., Slavin, J. A., et al., The Wind Magnetic Field Investigation, *Space Science Reviews*, 71, 207–229, 1995.
- Lugaz, N., Farrugia, C. J., Winslow, R. M., Al-Haddad, N., Galvin, A. B., et al., On the spatial coherence of magnetic ejecta: Measurements of coronal mass ejections by multiple spacecraft longitudinally separated by 0.01 au, *The Astrophysical Journal Letters*, 864, L7, 2018.
- Luhmann, J., Mewaldt, R., Cummings, A., Stone, E., Davis, A., et al., Stereo impact investigation goals, measurements, and data products overview, *Space Science Reviews*, 136, 2008.
- Maunder, M. L., Foullon, C., Forsyth, R., Barnes, D., and Davies, J., Multi-Spacecraft Observations of an Interplanetary Coronal Mass Ejection Interacting with Two Solar-Wind Regimes Observed by the Ulysses and Twin-STEREO Spacecraft, *Solar Physics*, 297, 148, 2022.
- Möstl, C., Weiss, A. J., Reiss, M. A., Amerstorfer, T., Bailey, R. L., et al., Multipoint interplanetary coronal mass ejections observed with Solar Orbiter, BepiColombo, Parker Solar Probe, Wind, and STEREO-A, *The Astrophysical Journal Letters*, 924, L6, 2022.
- Ogilvie, K. W., Chornay, D. J., Fritzenreiter, R. J., Hunsaker, F., Keller, J., et al., SWE, a comprehensive plasma instrument for the wind spacecraft, *Space Science Reviews*, 71, 55–77, 1995.
- Owen, C. J., Bruno, R., Livi, S., Louarn, P., Al Janabi, K., et al., The Solar Orbiter Solar Wind Analyser (SWA) suite, *Astronomy and Astrophysics*, 642, A16, 2020.
- Paschmann, G. and Daly, P. W., Analysis Methods for Multi-Spacecraft Data, *ISSI Scientific Reports Series*, 1, 1998.
- Pérez-Alanis, C. A., Janvier, M., Nieves-Chinchilla, T., Aguilar-Rodríguez, E., et al., Statistical Analysis of Interplanetary Shocks from Mercury to Jupiter, *Solar Physics*, 298, 60, 2023.
- Šafránková, J., Němeček, Z., Němec, F., Verscharen, D., Horbury, T. S., Bale, S. D., and Přejch, L., Evolution of magnetic field fluctuations and their spectral properties within the heliosphere: Statistical approach, *The Astrophysical Journal Letters*, 946, L44, 2023.
- Shi, C., Velli, M., Panasenco, O., Tenerani, A., Réville, V., et al., Alfvénic versus non-Alfvénic turbulence in the inner heliosphere as observed by Parker Solar Probe, *Astronomy and Astrophysics*, 650, A21, 2021.
- Smith, C., L'Heureux, J., Ness, N., Acuña, M., Burlaga, L., et al., The ace magnetic fields experiment, *Space Science Reviews*, 86, 613–632, 1998.
- Smith, C. W., Matthaeus, W. H., Zank, G. P., Ness, N. F., Oughton, S., and Richardson, J. D., Heating of the low-latitude solar wind by dissipation of turbulent magnetic fluctuations, *Journal of Geophysical Research: Space Physics*, 106, 8253–8272, 2001.
- Szabo, A., Koval, A., Kasper, J. C., Stevens, M., Case, A., et al., First Science Results from the DSCOVR Magnetometer, in *Solar Heliospheric and Interplanetary Environment (SHINE 2016)*, p. 9, 2016.
- Telloni, D., Spacecraft radial alignments for investigations of the evolution of solar wind turbulence: A review, *Journal of Atmospheric and Solar-Terrestrial Physics*, 242, 105 999, 2023.
- Torrence, C. and Compo, G. P., A Practical Guide to Wavelet Analysis., *Bulletin of the American Meteorological Society*, 79, 61–78, 1998.
- Trotta, D., Hietala, H., Horbury, T., Dresing, N., Vainio, R., et al., Multi-spacecraft observations of shocklets at an interplanetary shock, *Monthly Notices of the Royal Astronomical Society*, 520, 437–445, 2023.
- von Steiger, R. and Richardson, J. D., ICMEs in the Outer Heliosphere and at High Latitudes: An Introduction, *Space Science Reviews*, 123, 111–126, 2006.
- Zank, G. P., Nakanotani, M., Zhao, L. L., Du, S., Adhikari, L., et al., Flux ropes, turbulence, and collisionless perpendicular shock waves: High plasma beta case, *The Astrophysical Journal*, 913, 127, 2021.
- Zhao, L.-L., Zank, G. P., He, J. S., Telloni, D., Hu, Q., et al., Turbulence and wave transmission at an icme-driven shock observed by the solar orbiter and wind, *Astronomy and Astrophysics*, 656, A3, 2021.